UNIVERSITY OF WEST BOHEMIA

Applied and Computational Mechanics 2 (2008) 13–24

Applied and Computational Mechanics

Analysis of the conical piezoelectric acoustic emission transducer

O. Červená[a,*], P. Hora[a]

[a] *Institute of Thermomechanics of the ASCR, v.v.i., Veleslavínova 11, 301 14 Plzeň, Czech Republic*

Received 28 August 2008; received in revised form 2 October 2008

Abstract

Analyses of the properties of conical piezoelectric acoustic emission transducer are presented here. The conical piezoelectric transducer is used to scanning normal displacement on a surface of testing constructions in NDT methods, such as acoustic emission. The simplified one-dimensional analysis based on the equivalent circuit of conical waveguide is recapitulated. FEM analysis on this transducer is presented. Both the frequency response characteristic of the transducer and his time response on pulse excitation are results of this analysis. All of computations are done for various cone angles of piezoceramic (PTZ-H5) element and various sizes of the cylindrical backing of the sensor.

Keywords: acoustic emission, conical transducer, FEM

1. Introduction

A conical transducer is a highly sensitive wide-band device (operating up to several MHz) for measuring a vertical component of displacement of a small area on the surface of a body. This transducer is designed for a wide region of applications, e.g., for testing by means of acoustic emission, to be used as a standard transducer, and the like. The scheme of a conical transducer is shown in fig. 1. The basic characteristics of the transducer are as follows:
1) The active element is of piezoelectric ceramics and is conical and its polarization is parallel with the axis of the cone;
2) The greater base of the cone with scalded silver or gold electrode is soldered on a relatively great cylindrical backing block made usually from brass;
3) The smaller base of the cone with scalded silver or gold electrode is connected through the medium of as thin binding layer as possible with the part of relatively large surface on which is measured the vertical component of displacement;
4) The output voltage is measured between the brass cylindrical backing block and the surface of the active element.
5) The output voltage signal of a conical transducer is directly proportional to the normal surface displacement at the contact area with frequency up to few MHz.

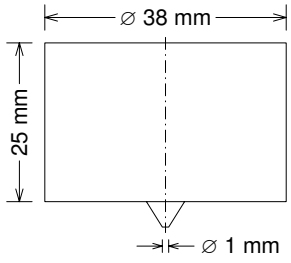

Fig. 1. A conical transducer

The conical transducers were developed by Proctor [7] in the 1980s for quantitative acoustic emission at the National Bureau of Standards (NBS), now the National Institute of Standards and Technology (NIST), USA.

*Corresponding author. Tel.: +420 377 236 415, e-mail: cervena@cdm.it.cas.cz.

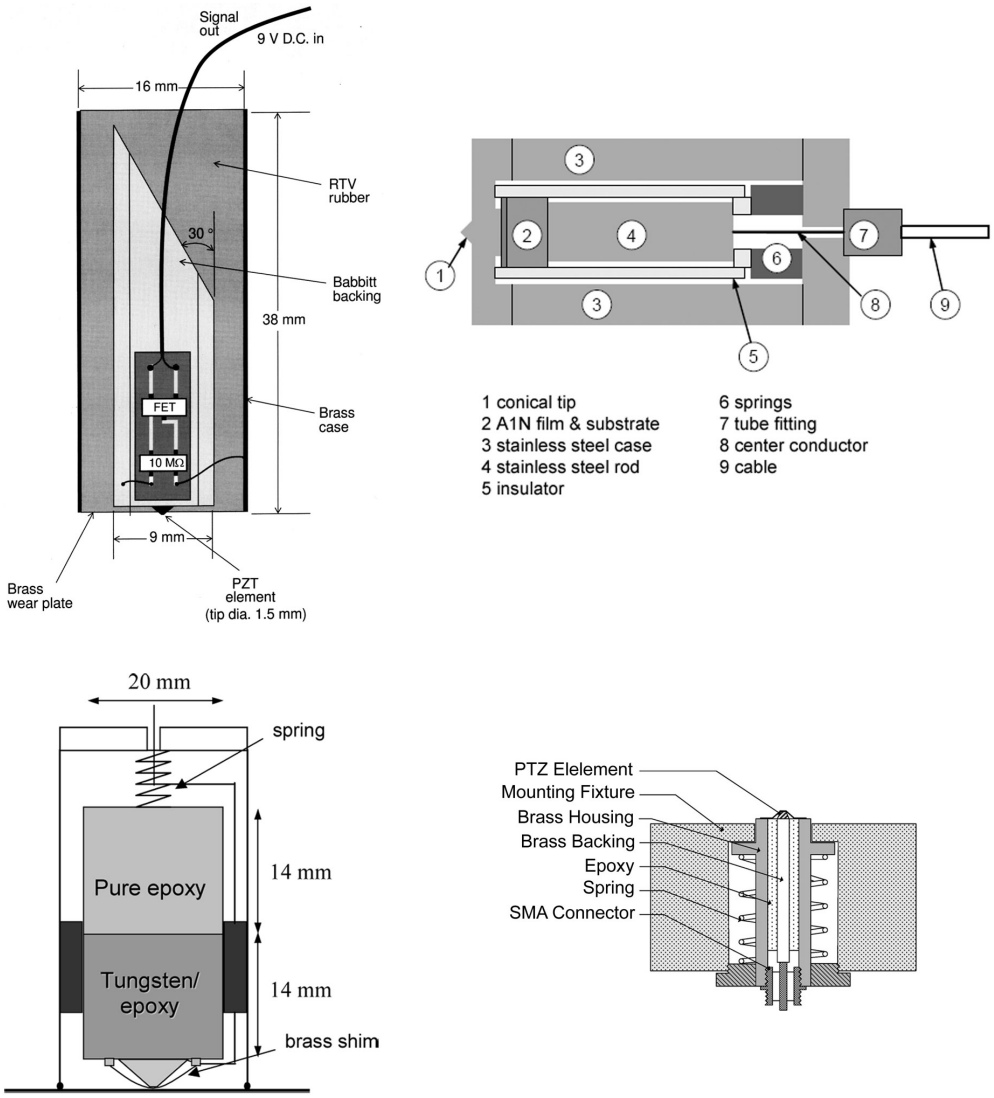

Fig. 2. Various kinds of conical transducers

There are many various transducers based on the NBS conical transducer. Some of them are shown in fig. 2. The top left image shows the unique embedded acoustic emission sensor used by Glaser [2]. The top right image shows the robust impact-echo sensor used by Sebastian [9]. The transducer was designed for continuous use up to at least $600\,^{\circ}\mathrm{C}$. The bottom left image shows the conical transducer used by Theobald [11] as an energy source for system calibration. The last image shows the new type miniature–conical transducer for acoustic emission measurements used by Lee [4].

1D analysis based on the model of the conical transducer developed by Greenspan [3] is presented in the second section. Greenspan extended the well-known Mason model [5] to account for the conical piezoelectric element. The third section deals with FEM analysis of the conical transducer.

2. One-dimensional analysis

Now we are going to determine an equivalent circuit of the conical transducer, and to calculate its frequency characteristic from geometrical dimensions and from material constants of an active element and terminal impedances.

By designing an equivalent circuit we will use as a basis an impedance matrix of a conical divergent waveguide, see fig. 3 — left in solid phase [5]

$$Z_m = \begin{bmatrix} \rho c S_1 \left(\dfrac{\cot(kl)}{i} + \dfrac{1}{ikx_1} \right) & -\rho c \sqrt{S_1 S_2} \dfrac{1}{i \sin(kl)} \\ \rho c \sqrt{S_1 S_2} \dfrac{1}{i \sin(kl)} & -\rho c S_2 \left(\dfrac{\cot(kl)}{i} - \dfrac{1}{ikx_2} \right) \end{bmatrix},$$

where ρ is a density, c is a phase velocity, i is imaginary unit, S_1, S_2 are areas of bases of a cone waveguide, k is wave number, l is the length and x_1, x_2 are parameters of a cone waveguide, see fig. 3 — left. This impedance matrix was derived on the assumption that the sections perpendicular to the axis of waveguide remain by deformation planar, the axial stress is uniformly distributed all over the surface and radial displacements can be neglected. Comparing the above relation with the matrix of T-element shown in fig. 3 — right,

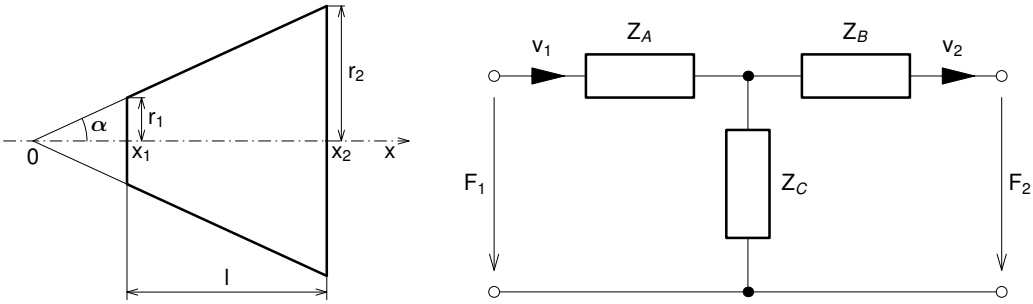

Fig. 3. A conical divergent waveguide (left), an equivalent circuit (right)

$$Z_T = \begin{bmatrix} Z_A + Z_C & -Z_C \\ Z_C & -Z_B - Z_C \end{bmatrix} \tag{1}$$

we get for Z_A, Z_B and Z_C the following relations

$$Z_A = \rho c S_1 \left(\frac{\cot(kl)}{i} + \frac{1}{ikx_1} - \frac{q}{i \sin(kl)} \right) \tag{2}$$

$$Z_B = \rho c S_2 \left(\frac{\cot(kl)}{i} - \frac{1}{ikx_2} - \frac{1/q}{i \sin(kl)} \right) \tag{3}$$

$$Z_C = \rho c \sqrt{S_1 S_2} \frac{1}{i \sin(kl)} \tag{4}$$

where $q = x_2/x_1 = r_2/r_1$.

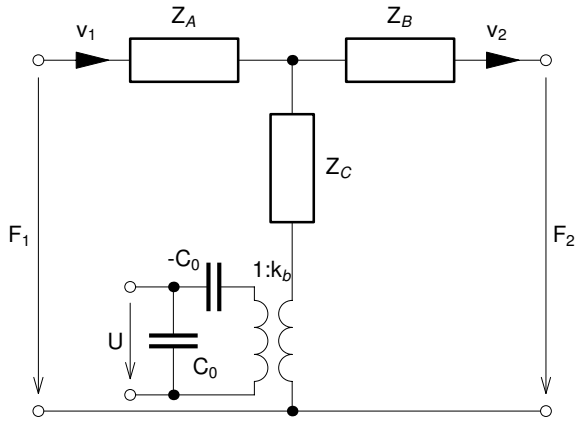

Fig. 4. Equivalent circuit of a conical piezoelectric element

If the T-element is supplemented by Mason's model, we get an equivalent circuit of a piezoelectric conical element, see fig. 4. Here k_b is a transformation ratio and C_0 is a transducer capacity.

Transferring the electric part to the mechanical side and on supplementing the circuit by source impedance Z_1 and load impedance Z_2 (see Norton's theorem — velocity short-circuited + parallel impedance Z_1), we get an equivalent circuit of a conic transducer, indicated in fig. 5. It should be remarked that v, v_1 and v_2 are loop velocities (not branch velocities), for instance, the velocity on Z_c is $v_1 - v_2$.

For the circuit shown in fig. 5 it holds

$$v_1 - v_2 = vF, \tag{5}$$

where

$$F = \frac{Z_1 \left(Z_B + Z_2\right)}{\left(Z_A + Z_1 + Z_C\right)\left(Z_B + Z_2 + Z_C\right) - Z_C^2} \tag{6}$$

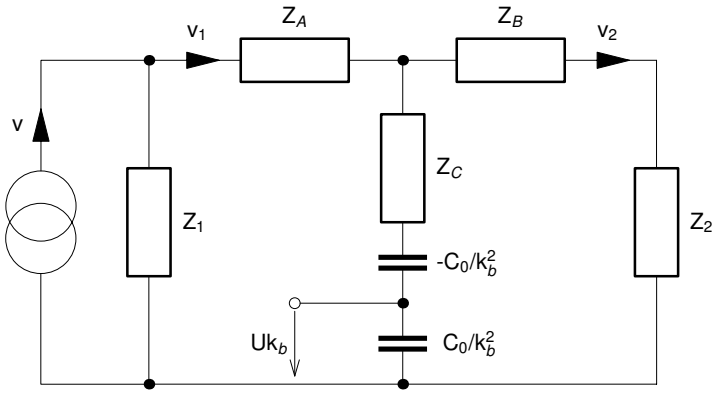

Fig. 5. Equivalent circuit of a conical transducer

and

$$Uk_b = \frac{v_1 - v_2}{i\omega C_0/k_b^2}. \tag{7}$$

On substituting for $v_1 - v_2$ from equation (5) into equation (7), we obtain

$$Uk_b = \frac{v}{i\omega}\frac{k_b^2}{C_0}F. \tag{8}$$

Further, substituting $\xi = v/i\omega$ and $-p_{33} = k_b/C_0$ we get

$$U/\xi = -p_{33}F, \tag{9}$$

which is the resultant relation for sensitivity of a conical transducer.

The value of p_{33} lies between h_{33} (disc) and g_{33}/s_{33}^D (rod). h_{33} is piezoelectric constant (for calculation we used the value $21.5 \cdot 10^8$ V/m). g_{33} is piezoelectric constant (for calculation we used the value $24.9 \cdot 10^{-3}$ Vm/N) and s_{33}^D is the yielding constant at $D = 0$ (for calculation we used the value $9.46 \cdot 10^{-12}$ m^2/N).

Substituting relations (2)–(4) into relation (6) for individual impedances, we get the numerator of fraction F

$$N_F = z_1\left[z_2 + i\left(\frac{1}{q\sin(kl)} + \frac{q-1}{qkl} - \cot(kl)\right)\right] \tag{10}$$

and denominator of fraction F

$$\begin{aligned} D_F = 1 + z_1 z_2 + \frac{(q-1)^2}{q(kl)^2} - \frac{(q-1)^2}{qkl}\cot kl + \\ + i\left[z_1\left(\frac{q-1}{qkl} - \cot(kl)\right) - z_2\left(\frac{q-1}{kl} + \cot(kl)\right)\right]. \end{aligned} \tag{11}$$

Here z_1 and z_2 are scaled specific impedances $Z_1/\rho c S_1$ and $Z_2/\rho c S_2$ (the scaling is carried out to ρc of the cone!).
In the case of the cylindrical transducer, $q = 1$, we get for F

$$F = \frac{z_1\left[z_2 + i\tan(kl/2)\right]}{1 + z_1 z_2 - i\left(z_1 + z_2\right)\cot(kl)}. \tag{12}$$

For kl an odd multiple of π, the numerator and denominator in equation (12) are both infinite, but the ratio is finite; however, for kl a multiple of 2π, i.e., if length l is equal to integral multiple of wave length, the denominator is infinite for any z_1 and z_2, hence, both F and sensitivity U/ξ are zero. For the case of a cone, the expression $1/\left(q\sin(kl)\right)$ for $q > 1$ preserves the finite value of fraction F in equation (6). Instead of zeros, in this case, there are only minima in the characteristic. This is the reason why a conical transducer yields a suitably even wide-band characteristic (which cannot be achieved with a cylindrical transducer), see fig. 6.

In practical applications the signals detected by a conic transducer are so short that both the test medium and the backing may be supposed to be half–spaces. The problem of the impedance in a half-space (values of Z_1 and Z_2), considered in a circular area with radius a on the surface of a half-space, was solved in [3].

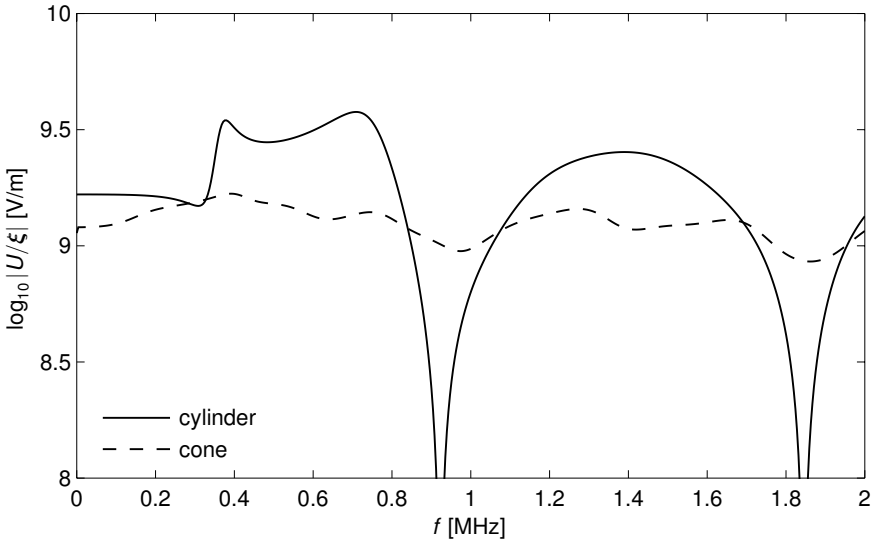

Fig. 6. Frequency dependencies of sensitivity for cylindrical ($r_1 = r_2 = 0.5$, $l = 4$ mm) and conical transducer ($r_1 = 0.5$, $r_2 = 3$, $l = 4$ mm)

3. FEM analysis

FEM calculations were performed in the commercial environment COMSOL Multiphysics [1]. Because of the axial symmetry of the geometry, an axisymmetric 2D application mode was used. Elements were the Lagrange-Quadratic type. It was used the linear system solver, direct (UMFPACK).

Computations were performed for nine various piezoelectric element sizes, see tab. 1–left. The parameters in this table correspond to labelling in fig. 3 — left and q is a ratio of radii of the cone. The influence of the backing size was studied on four various examples, see tab. 1 — right.

Table 1. Transducer parameters: element (left), backing (right)

element					
Type	r_1 [mm]	r_2 [mm]	q [–]	l [mm]	α [deg]
cylinder	0.5	0.5	1	4.0	0.00
cone 10	0.5	1.0	2	4.0	7.13
cone 15	0.5	1.5	3	4.0	14.04
cone 20	0.5	2.0	4	4.0	20.56
cone 25	0.5	2.5	5	4.0	26.57
cone 30	0.5	3.0	6	4.0	32.01
cone 35	0.5	3.5	7	4.0	36.87
cone 40	0.5	4.0	8	4.0	41.19
cone 45	0.5	4.5	9	4.0	45.00

backing		
Type	height [mm]	radius [mm]
A	25.0	3.0
B	25.0	11.0
C	12.5	19.0
D	25.0	19.0

Material of piezoelectric elements was lead zirconate titanate (PZT-5H) with parameters:
elasticity matrix

$$c = \begin{bmatrix} 127.205 & 80.212\,2 & 84.670\,2 & 0 & 0 & 0 \\ 80.212\,2 & 127.205 & 84.670\,2 & 0 & 0 & 0 \\ 84.670\,2 & 84.670\,2 & 117.436 & 0 & 0 & 0 \\ 0 & 0 & 0 & 22.988\,5 & 0 & 0 \\ 0 & 0 & 0 & 0 & 22.988\,5 & 0 \\ 0 & 0 & 0 & 0 & 0 & 23.474\,2 \end{bmatrix} \text{GPa},$$

coupling matrix (stress-charge form)

$$e = \begin{bmatrix} 0 & 0 & 0 & 0 & 17.034\,5 & 0 \\ 0 & 0 & 0 & 17.034\,5 & 0 & 0 \\ -6.622\,81 & -6.622\,81 & 23.240\,3 & 0 & 0 & 0 \end{bmatrix} \text{C/m}^2,$$

permittivity matrix (stress-charge form)

$$\varepsilon_S = \begin{bmatrix} 1\,704.4 & 0 & 0 \\ 0 & 1\,704.4 & 0 \\ 0 & 0 & 1\,433.6 \end{bmatrix},$$

and density $\rho = 7\,500\,\text{kg/m}^3$.

The transducer backing was created by brass with Young's modulus $E = 110\,\text{GPa}$, Poisson's ratio $\nu = 0.35$ and density $\rho = 8\,700\,\text{kg/m}^3$.

Two kinds of problems were realized. Firstly, the frequency response analysis, and secondly, the time dependent analysis. A mapped mesh consisting of quadrilateral elements was created in both cases. But size of elements was different.

The following boundary conditions were set for both of cases. The numbering of boundaries is presented in fig. 7. The constraint was given by prescribed displacement on boundary 2 and on the other boundaries it was free. The electric boundary conditions were axial symmetry on boundary 1, ground on boundary 2 and zero charge on boundary 6.

The boundary integration variable V_{int} was defined on boundary 4 as $V_{int} = V2\pi r$, here V is a voltage and r is a radius.

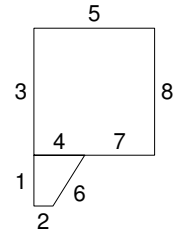

Fig. 7. Boundary

3.1. Frequency response analysis

The maximal size of one mesh element was $0.5 \times 0.5\,\text{mm}$. The amplitude of the prescribed displacement (in axis of symmetry-direction) on boundary 2 (see fig. 7) was 1 pm. The Rayleigh damping was used with mass damping parameter $\alpha_{dM} = 209\,440\,\text{s}^{-1}$ and stiffness damping parameter $\beta_{dK} = 1.06 \cdot 10^{-8}\,\text{s}$. It was solved frequency response by parametric solver. The excitation frequency was in range from 10^3 to 10^6 with step 10^3 Hz. We studied the response of voltage U ($U = V_{int}/(\pi r_2^2)$) on boundary 4, see fig. 7.

The analysis was performed both for whole transducers and for separate piezoelectric elements. It was always done for nine shapes of cone (see tab. 1 — left). Because some very similar jobs were performed, we used advantageously MATLAB [10] for scripting these tasks of COMSOL. We created three scripts. The first one was for whole transducers, the second one for separate elements and the third one was for transducer with the "cone 30" element and four various sizes of backing (tab. 1). We defined in those scripts mapped mesh, materials, boundary conditions, boundary integration variable V_{int}, damping and excitation frequency. The problem was solved for particular shapes of geometry, which we changed in loop.

The fig. 8 — top displays the frequency responses of transducers with backing D for particular piezoelectric element types (tab. 1). The curves get smoother the bigger a ratio of the element radii is. The fig. 8 — bottom shows the frequency response of transducer elements only (without backing). By comparing these figures it is evident that using of the backing in transducers is necessary.

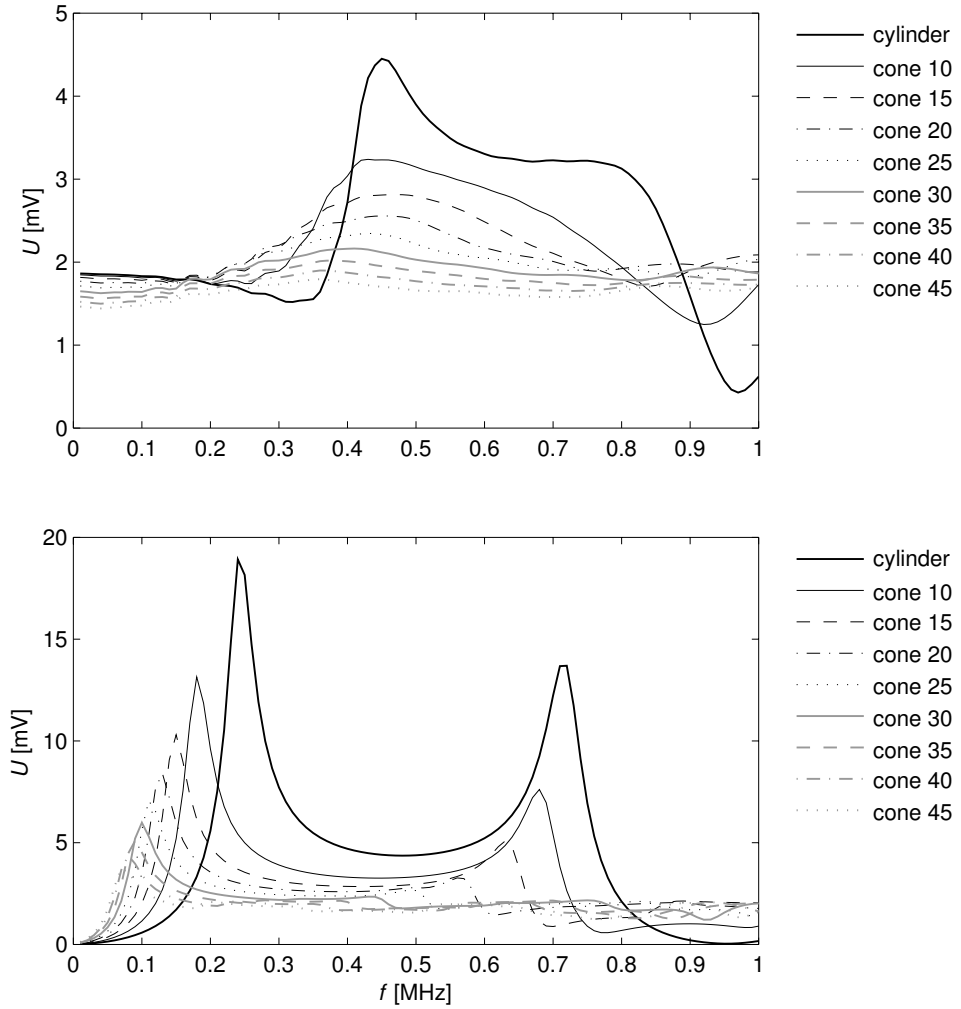

Fig. 8. Frequency responses of transducers (top) and elements (bottom)

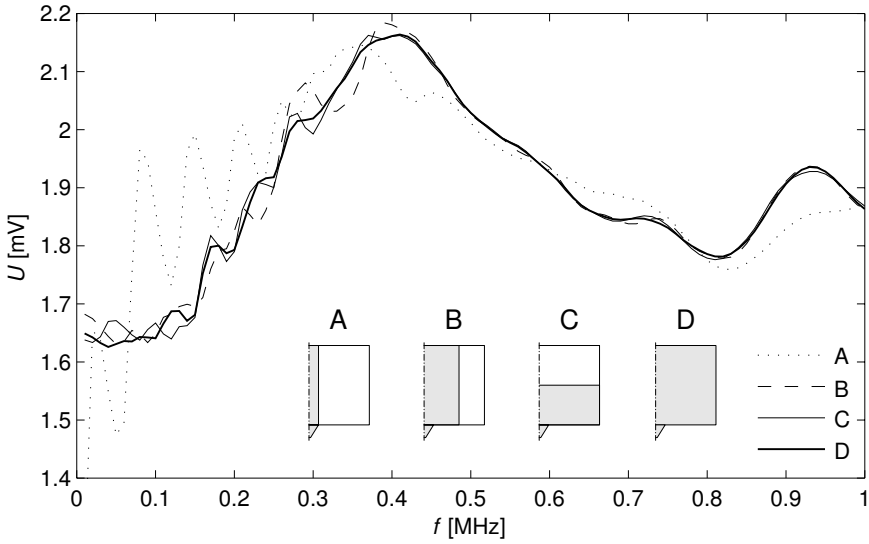

Fig. 9. Influence of backing geometry on the frequency response

The fig. 9 shows influence of backing shape on the frequency response. The backing geometry A, B, C and D is given in tab. 1 — right. The piezoelectric element with the "cone 30" (tab. 1 — left) was used in all cases. Note, the radius of backing influences more the frequency response of transducer than the height of backing.

3.2. Time dependence analysis

The maximal size of one mesh element was 0.25×0.25 mm. No damping and backing D was used in the time dependence problems. The time stepping parameters were: times (from 0 to 50 with step $0.01\,\mu$s), relative tolerance (10^{-5}) and absolute tolerance (10^{-10}). We studied the response of voltage U ($U = V_{int}/(\pi r_2^2)$) on boundary 4 (see fig. 7) as well as for the frequency response analysis.

The prescribed displacement on boundary 2 (see fig. 7) was given by a function or a data file. The sinus-pulse-displacement function had amplitude 1 pm, frequency 2 MHz and width $0.5\,\mu$s, see fig. 10.

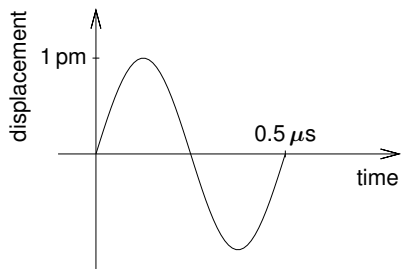

Fig. 10. A sinus — pulse function

A relative frequency response can be determined by dividing the Fourier transform of the time waveform produced by the transducer by the Fourier transform of the prescribed time waveform, see fig. 11. The frequency response obtained by the Fourier transform (fig. 11 — bottom) is in a good agreement with that obtained by 1D analysis (fig. 6).

The data file with the prescribed displacement on boundary 2 (see fig. 7) included the vertical displacement on surface of half-space in distance 2 cm from the step-point-force source, [6]. The force amplitude was 10 N.

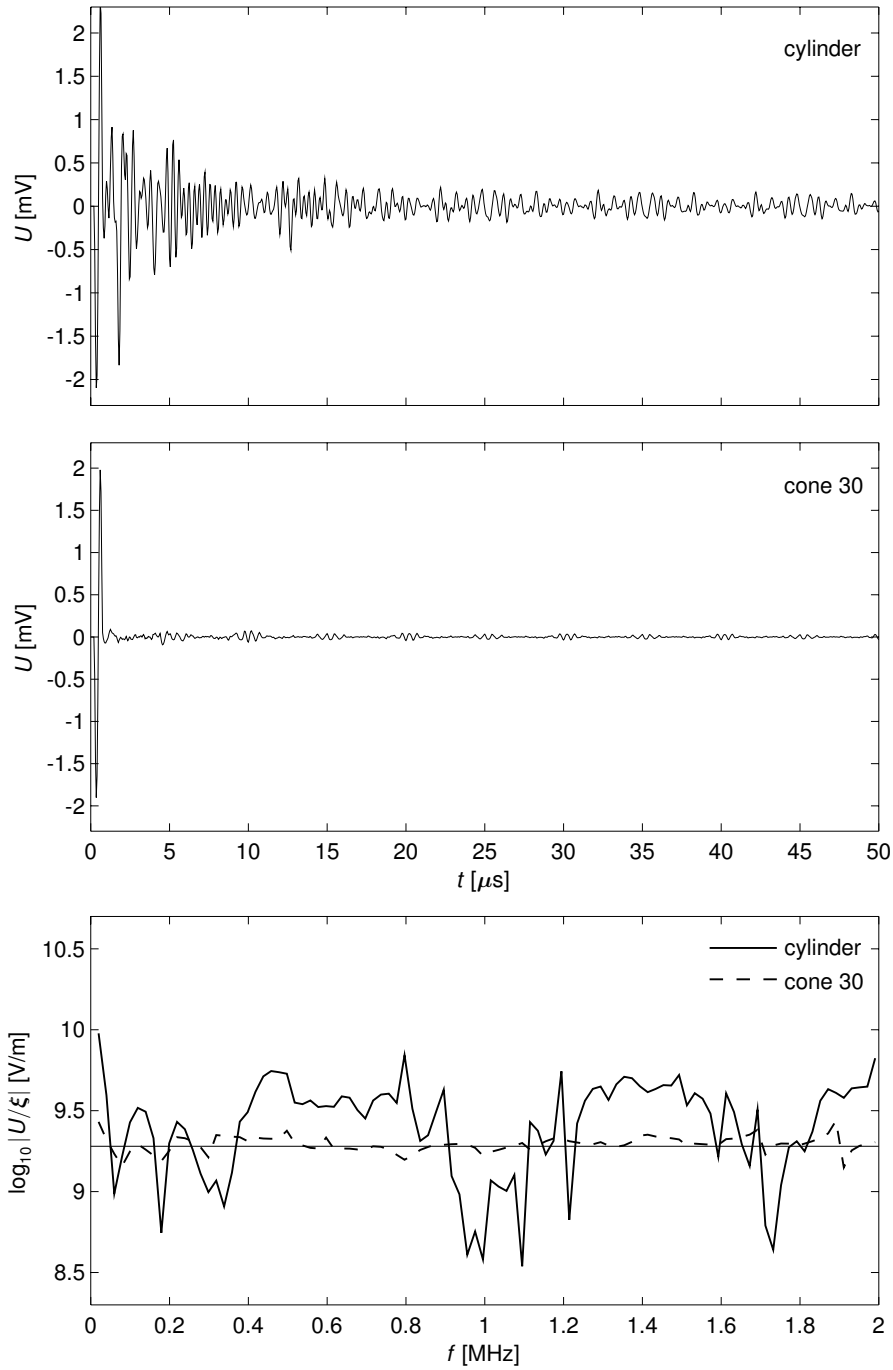

Fig. 11. The pulse time response of cylinder (top), cone (middle) transducer and their frequency responses (bottom). Thin line in bottom image notes mean value of frequency response for the "cone 30" transducer

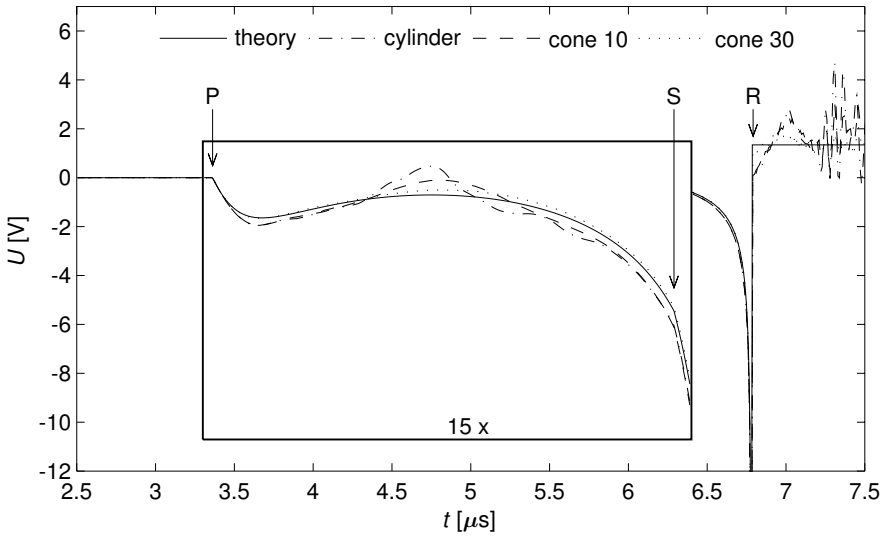

Fig. 12. The theoretical waveform and the pulse time response of cylinder, "cone 10", "cone 30" transducer

The time response of cylinder, "cone 10" and "cone 30" transducer on the step-point-force source are shown in fig. 12. The theoretical displacement waveform multiplied by the transducer sensitivity ($1.9 \cdot 10^9$ V/m) is added to these time responses. The value $1.9 \cdot 10^9$ was taken from fig. 11 — bottom as a mean value of sensitivity for the "cone 30" transducer ($\log_{10} 1.9 \cdot 10^9 \doteq 9.28$). As shown, the "cone 30" transducer signal is almost exactly as predicted by theory. The letters P, S and R in the figure noted the arrival time of longitudinal (primary), transverse (secondary) and Rayleigh wave, respectively.

4. Conclusion

Analyses of the properties of conical piezoelectric acoustic emission transducer were presented. The conical piezoelectric transducer is used to scanning normal displacement on a surface of testing constructions in NDT methods, such as acoustic emission. The simplified 1D analysis based on the equivalent circuit of conical waveguide was recapitulated. FEM analysis of this transducer was presented. Both the frequency response characteristic of the transducer and his time response on pulse excitation were studied. All of computations were done for various cone angles of piezoceramic (PTZ-H5) element and various sizes of the cylindrical backing of transducer.

FEM calculations were performed in the environment COMSOL Multiphysics [1] with MATLAB [10] (for scripting of COMSOL tasks).

The 1D analysis explained the normal mode degeneracies of the usual cylindrical piezoelectric disk element. The FEM analysis showed necessity of using the large transducer backing. The radius of backing influences more the frequency response of transducer than the height of backing. It was shown in the time dependence analysis that the "cone 30" transducer signal is almost exactly as predicted by theory.

A transducer for measuring tangential dynamic displacement of a transient nature at a point location on the surface of a mechanical body was patented by Proctor [8]. Our next goal will be the FEM analysis of this transducer. Further we consider supplementing FEM analysis of the conical transducer by horizontal excitation. Both of these tasks require full 3D analysis, which poses considerable claims of the computer technique parameters.

Acknowledgements

The work was supported by the Czech Science Foundation under the grant 101/06/1689 and the research project AV0Z20760514 of AS CR.

References

[1] COMSOL, Inc., http://www.comsol.com

[2] S. D. Glaser, G. G. Weiss, L. R. Johnson, Body waves recorded inside an elastic half-space by an embedded, wideband velocity sensor, J. Acoust. Soc. Am. 104 (3) (1998) 1 404–1 412.

[3] M. Greenspan, The NBS conical transducer: Analysis, J. Acoust. Soc. Am. 81 (1) (1987) 173–183.

[4] Y. C. Lee, Z. Lin, Miniature piezoelectric conical transducer: Fabrication, evaluation and application, Ultrasonics 44 (2006) e693–e697.

[5] A. Mohamed, Equivalent circuits of solid horns undergoing longitudinal vibration, J. Acoust. Soc. Am. 38 (1965) 862–866.

[6] H. M. Mooney, Some numerical solutions for Lamb's problem, B. Seism. Soc. Am. 64 (1974) 473–491.

[7] T. M. Proctor Jr., An improved piezoelectric acoustic emission transducer, J. Acoust. Soc. Am. 71 (5) (1982) 1 163–1 168.

[8] T. M. Proctor Jr., Transducer for measuring transient tangential motion, United States Patent, Patent Number: 4782701.

[9] J. Sebastian, Monitoring of refractory wall recession using high-temperature impact-echo instrumentation, UDRI University of Dayton, Research institute, Dayton, 2004.

[10] The MathWorks, Inc., http://www.mathworks.com

[11] P. D. Theobald, Towards traceable calibration of acoustic emission measurement systems: development of a reference source at the UK's National Physical Laboratory, DGZfP-Proceedings BB 90-CD, DGZfP-Proceedings BB 90-CD, EWGAE, 72, 2004, pp. 683–690.